

Original Research

Synthesis, SAR and biological evaluation of a novel series of 1-(2-chloroethyl)-1-nitroso-3-(2-(3-oxobenzoelenazol-2(3H)-yl)ethyl) urea: Organoselenium compounds for cancer therapy

S. Ye^{1,2}, X. Zheng^{1,2}, T. Hu^{1,2}, H. Zeng^{1,2*}

¹ State Key Laboratory of Natural and Biomimetic Drugs, Peking University, Beijing 100191, China

² School of Pharmaceutical Sciences, Peking University, Beijing 100191, China

Abstract: Thioredoxin reductase 1 (TrxR1) is an important potential anticancer drug target and closely related to both carcinogenesis and cancer progression. Ehaselen (BBSKE), a novel organoselenium compound inhibiting TrxR1 with selective antitumor effect, while its symmetrical structure results in poor solubility. Carmustine (BCNU), a DNA cross-link agent and also a deactivator of TrxR, is with high toxicity and low selectivity which limit its clinical application to some extents. Herein, a novel compound, 1-(2-chloroethyl)-1-nitroso-3-(2-(3-oxobenzoelenazol-2(3H)-yl)ethyl)urea(4a-1), which was designed through the combination of Ehaselen and Carmustine, showed good solubility, good targetability, low toxicity and excellent antitumor activity by synergism. Using the structure of 4a-1 as a key active scaffold, a series of novel 1-(2-chloroethyl)-1-nitroso-3-(2-(3-oxobenzoelenazol-2(3H)-yl)ethyl)urea was designed, synthesized and evaluated to explore the structure–activity relationships (SARs) of these inhibitors and to improve their antitumor activities. Notably, 1-(2-chloroethyl)-3-(2-(6-fluoro-3-oxobenzoselenazol-2(3H)-yl)ethyl)-1-nitrosourea(4b-1) was found to exhibit more potent antitumor activities comparable to 4a-1 against all the four cancer cell lines, including Mia PaCa-2, PANC-1, RKO, LoVo. These results have highlighted compound 4b-1 as a new potential lead candidate for future development of novel potent broad-spectrum antitumor agents. In addition, a SAR model was established to conduct further structural modification.

Key words: Ehaselen, Carmustine, thioredoxin reductase, synergism, inhibitor, toxicity, solubility, targetability, antitumor, SAR.

Introduction

Thioredoxin reductase (TrxR), a selenoprotein, is one of the major antioxidant and redox regulators in mammals that is expressed in all types and organs (1-3). However, compared to the normal cells, the level of TrxR is often more than 10-fold greater in the malignant cells (4, 5). It has been implicated that TrxR is a promising target for anticancer drug design (5, 6). The conserved C-terminal sequences (-GCUG-) of TrxR, acts as the key catalytically active part which is easily combined with a wide of substrates (7). Ehaselen, entered phase II clinical trials in China, prepared by our lab, was demonstrated (8-10) to be a good inhibitor of TrxR. Targeted the active sites of Cys497 and Sec498 of TrxR, Ehaselen showed remarkable anticancer potency in both vitro and vivo (8-11). However, the symmetrical structure of Ehaselen leads to poor solubility.(12) Carmustine, a DNA cross-link agent (13, 14) and also a deactivator of TrxR (15,16), is with high toxicity (17-19) and low selectivity which limited its clinical application to some extents.

Herein, using the combination principles, 1-(2-chloroethyl)-1-nitroso-3-(2-(3-oxobenzoselenazol-2(3H)-yl)ethyl)urea (4a-1) was designed with the both essential parts for activities of Ehaselen and carmustine retained as shown in Figure 1. The two essential parts of 4a-1 from the parental compound were combined as a complementary design for good solubility, good target ability, and low toxicity and effected as synergism of antitumor mechanism. With the purpose of exploring any the structure–activity relationships (SARs) of the inhibitors, using the structure of 4a-1 as an important

starting point, a class of novel 1-(2-chloroethyl)-1-nitroso-3-(2-(3-oxobenzoelenazol-2(3H)-yl)ethyl)urea was designed and synthesized. Solubility and toxicity evaluations of target compounds were carried out to assess the improved properties as designed. In order to investigate the target ability and efficacy as an antitumor compound, the inhibition correlation between TrxR and cell growth were studied. Docking studies of 4b-1 as a representative candidate were also conducted.

Materials and Methods

Chemicals and methods

¹H and ¹³C NMR spectra were recorded on a Bruker Avance III instrument, 400 MHz for ¹H spectra and

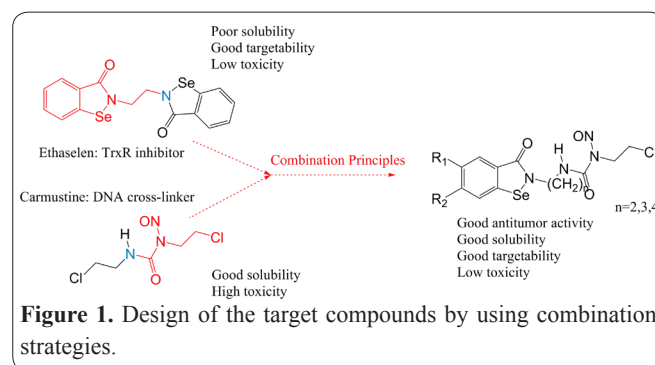


Figure 1. Design of the target compounds by using combination strategies.

Received April 22, 2016; Accepted May 27, 2016; Published June 30, 2016

* Corresponding author: Huihui Zeng, Health Science Center, Peking University, Beijing 100191, China. Email: zenghh@bjmu.edu.cn

Copyright: © 2016 by the C.M.B. Association. All rights reserved.

100 MHz for ^{13}C spectra, in DMSO-d_6 or CDCl_3 . The chemical shifts are reported in δ (ppm) relative to tetramethylsilane as the internal standard. Mass spectra were recorded using APEX IV FT-MS (7.0T). All chemical reagents and solvents used in this paper were purchased from Sigma–Aldrich, Alfa Aesar and TCI in high quality.

Synthesis

General methods of the synthesis of 2(a–h)

0.1 mol 2-Amino benzoic acid dissolved in HCl aqueous solution (50%, 40ml) and dropwise added an aqueous solution of sodium nitrite (30%, 0.12 mol) under 0°C . After 1h reaction, an aqueous solution of disodium diselenide (0.05 mol) was added into the reaction system and stirred for another 2h at 20°C . The aqueous HCl (10%) were used to adjust PH of the system to a value of 2. Then, the final products were precipitated and obtained by filtration.

2,2'-diselanediyldibenzoic acid (2a)

Compound 1a (13.7 g, 0.1 mol) was used as reactant to give 19.4 g of 2a as yellow solid (94%). ^1H NMR (400 MHz, DMSO-d_6) δ 13.67 (br, 2H, COOH), 8.00 (d, J = 7.6 Hz, 2H, ArH), 7.66 (d, J = 7.6 Hz, 2H, ArH), 7.45 (t, J = 7.6 Hz, 2H, ArH), 7.33 (t, J = 7.6 Hz, 2H, ArH). ^{13}C NMR (100 MHz, DMSO-d_6) δ 168.62, 133.43, 133.15, 131.41, 129.65, 129.43, 126.32. MS (EI) m/z: 401.9 (M+).

6,6'-diselanediyldibis(3-fluorobenzoic acid) (2b) Compound 1b (15.5 g, 0.1 mol) was used as reactant to give 18.0 g of 2b as yellow solid (82%). ^1H NMR (400MHz, DMSO-d_6) δ 14.07 (br, 2H, COOH), 7.78 (dd, J1 = 9.1, J2 = 2.8, 2H, ArH), 7.65 (dd, J1 = 8.5, J2 = 5.2, 2H, ArH), 7.42 (td, J1 = 8.5, J2 = 2.8, 2H, ArH). ^{13}C NMR (100MHz, DMSO-d_6) δ 167.54, 160.91 (d, JC–F = 244.5), 131.65 (d, JC–F = 7.2), 130.34 (d, JC–F = 6.7), 128.18 (d, JC–F = 2.5), 120.96 (d, JC–F = 21.6), 117.85 (d, JC–F = 23.0). MS (EI) m/z: 437.9 (M+).

2,2'-diselanediyldibis(4-fluorobenzoic acid) (2c) Compound 1c (15.5 g, 0.1 mol) was used as reactant to give 15.4 g of 2c as yellow solid (70%). ^1H NMR (400 MHz, DMSO-d_6) δ 13.92 (br, 2H, COOH), 8.12 (dd, J1 = 8.4, J2 = 6.0, 2H, ArH), 7.40 (dd, J1 = 9.8, J2 = 2.3, 2H, ArH), 7.23 (td, J1 = 8.4, J2 = 2.3, 2H, ArH). ^{13}C NMR (100MHz, DMSO-d_6) δ 167.76, 162.52 (d, JC–F = 250.5), 136.64 (d, JC–F = 8.5), 134.46 (d, JC–F = 20.8), 125.77 (d, JC–F = 9.3), 116.09 (d, JC–F = 3.5), 114.05 (d, JC–F = 25.0). MS (EI) m/z: 438.0 (M+).

6,6'-diselanediyldibis(3-chlorobenzoic acid) (2d) Compound 1d (17.1 g, 0.1 mol) was used as reactant to give 18.6 g of 2d as yellow solid (79%). ^1H NMR (400MHz, DMSO-d_6) δ 14.12 (br, 2H, COOH), 8.00 (d, J = 2.2, 2H, ArH), 7.64 (d, J=8.6, 2H, ArH), 7.60 (dd, J1 = 8.6, J2 = 2.2, 2H, ArH). ^{13}C NMR (100MHz, DMSO-d_6) δ 167.92, 144.59, 133.82, 132.55, 132.04, 131.26, 130.89. MS (EI) m/z: 469.8 (M+).

2,2'-diselanediyldibis(4-chlorobenzoic acid) (2e) Compound 1e (17.1 g, 0.1mol) was used as reactant to give 19.1 g of 2e as yellow solid (81%). ^1H NMR (400MHz,

DMSO-d_6) δ 14.08 (br, 2H, COOH), 8.03 (d, J = 8.3, 2H, ArH), 7.60 (d, J = 1.7, 2H, ArH), 7.44 (dd, J1 = 8.3, J2 = 1.7, 2H, ArH). ^{13}C NMR (100 MHz, DMSO-d_6) δ 171.56, 150.02, 137.26, 137.07, 133.18, 129.34, 125.58. MS (EI) m/z: 469.9 (M+).

6,6'-diselanediyldibis(3-methylbenzoic acid) (2f) Compound 1f (15.1 g, 0.1 mol) was used as reactant to give 19.5 g of 2f as yellow solid (86%). ^1H NMR (400 MHz, DMSO-d_6) δ 13.55 (br, 2H, COOH), 7.84 (d, J = 1.4 Hz, 2H, ArH), 7.50 (d, J=8.2 Hz, 2H, ArH), 7.29 (dd, J1 = 8.2Hz, J2=1.4 Hz, 2H, ArH), 2.29 (s, 6H, CH3). ^{13}C NMR (100 MHz, DMSO-d_6) δ 168.52, 135.94, 134.33, 131.82, 129.84, 129.45, 128.52, 20.07. MS (EI) m/z: 429.9 (M+).

6,6'-diselanediyldibis(3-methoxybenzoic acid) (2g) Compound 1g (4.3 g, 0.01 mol) was used as reactant to give 2.1 g of 2g as yellow solid (46%). ^1H NMR (400 MHz, DMSO-d_6) δ 12.13 (br, 2H, COOH), 7.60 (d, J = 8.8, 2H, ArH), 7.20 (d, J = 2.7, 2H, ArH), 7.13 (dd, J1 = 8.8, J2 = 2.7, 2H, ArH), 3.75 (s, 6H, OCH3). ^{13}C NMR (100 MHz, DMSO-d_6) δ 168.20, 158.18, 130.75, 129.64, 123.26, 120.22, 115.96, 55.52. MS (ESI) m/z: 460.9 (M+_H).

6,6'-diselanediyldibis(3-bromobenzoic acid) (2h) Compound 1h (21.5 g, 0.1 mol) was used as reactant to give 19.4 g of 2h as yellow solid (69%). ^1H NMR (400MHz, DMSO-d_6) δ 14.06 (br, 2H, COOH), 8.10 (d, J = 2.3, 2H, ArH), 7.69 (dd, J1 = 8.6, J2 = 2.3, 2H, ArH), 7.55 (d, J = 8.6, 2H, ArH). ^{13}C NMR (100MHz, DMSO-d_6) δ 171.55, 145.11, 138.92, 136.65, 130.36, 128.77, 120.31. MS (EI) m/z: 557.7 (M+).

General methods of the synthesis of 3(a–h)

2,2'-diselanediyldibenzoic acid (0.01 mol) was added to thionyl chloride (20 ml) and the reaction was catalyzed by DMF (0.5 ml). The mixture was stirred at reflux (85°C) for 3 h. The solvents were evaporated under vacuum and the crude products were purified by recrystallization from cyclohexane.

2-(chlorocarbonyl)phenyl hypochloroselenoite (3a) Compound 2a (4g, 0.01 mol) was used as reactant to give 3.9 g of 3a as orange crystal (79%). ^1H NMR (400 MHz, CDCl_3) δ 8.09 (d, J = 7.7, 1H, ArH), 7.85 (d, J = 7.7, 1H, ArH), 7.67 (t, J = 7.7, 1H, ArH), 7.39 (t, J = 7.7, 1H, ArH). ^{13}C NMR (100 MHz, CDCl_3) δ 164.51, 136.19, 134.54, 131.29, 129.03, 127.41, 126.42.

2-(chlorocarbonyl)-4-fluorophenyl hypochloroselenoite (3b)

Compound 2b (4.4 g, 0.01 mol) was used as reactant to give 4.0 g of 3b as orange crystal (70%). ^1H NMR (400 MHz, CDCl_3) δ 7.78 (dd, J1 = 9.0, J2 = 2.7, 1H, ArH), 7.65 (dd, J1 = 8.3, J2 = 5.4, 1H, ArH), 7.42 (td, J1 = 8.3, J2 = 2.7, 1H, ArH). ^{13}C NMR (100 MHz, CDCl_3) δ 168.84, 161.41 (d, JC–F = 248.6), 131.65 (d, JC–F = 7.5), 130.34 (d, JC–F = 8.7), 128.18 (d, JC–F = 2.2), 120.96 (d, JC–F = 24.3), 117.85 (d, JC–F = 22.5).

2-(chlorocarbonyl)-5-fluorophenyl hypochloroselenoite (3c)

Compound 2c (4.4 g, 0.01 mol) was used as reactant to give 4.3 g of 3c as orange crystal (80%). ¹H NMR (400 MHz, CDCl₃) δ 7.86 (dd, J₁ = 9.9, J₂ = 2.3, 1H, ArH), 7.80 (dd, J₁ = 8.4, J₂ = 5.7, 1H, ArH), 7.19 (td, J₁ = 8.4, J₂ = 2.3, 1H, ArH). ¹³C NMR (100 MHz, CDCl₃) δ 171.83, 160.44, 147.83, 144.46, 135.26, 127.44, 127.10.

4-chloro-2-(chlorocarbonyl)phenyl hypochloroselenoite (3d)

Compound 2d (4.7g, 0.01mol) was used as reactant to give 4.0g of 3d as orange crystal (76%). ¹H NMR (400 MHz, CDCl₃) δ 8.12 (d, J = 8.6, 1H, ArH), 7.69 (d, J = 2.2, 1H, ArH), 7.65 (dd, J₁ = 8.6, J₂ = 2.2, 1H, ArH). ¹³C NMR (100MHz, CDCl₃) δ 171.70, 144.40, 136.12, 133.58, 133.06, 130.02, 128.51.

5-chloro-2-(chlorocarbonyl)phenyl hypochloroselenoite (3e)

Compound 2e (4.7g, 0.01mol) was used as reactant to give 4.8g of 3e as orange crystal (83%). ¹H NMR (400 MHz, CDCl₃) δ 8.13 (d, J = 1.8, 1H, ArH), 7.74 (d, J = 8.1, 1H, ArH), 7.40 (dd, J₁ = 8.1, J₂ = 1.8, 1H, ArH). ¹³C NMR (100 MHz, CDCl₃) δ 171.61, 151.20, 136.24, 135.47, 132.15, 128.54, 124.58.

2-(chlorocarbonyl)-4-methylphenyl hypochloroselenoite (3f)

Compound 2f (4.3 g, 0.01 mol) was used as reactant to give 4.4 g of 3f as orange crystal (81%). ¹H NMR (400 MHz, CDCl₃) δ 7.96 (d, J = 8.2, 1H, ArH), 7.65 (s, 1H, ArH), 7.48 (d, J = 8.2, 1H, ArH), 2.37 (s, 6H, CH₃). ¹³C NMR (100MHz, CDCl₃) δ 172.74, 141.63, 135.72, 134.17, 129.61, 127.44, 126.38, 20.66.

2-(chlorocarbonyl)-4-methoxyphenyl hypochloroselenoite (3g)

Compound 2g (5.2 g, 0.01 mol) was used as reactant to give 3.7 g of 3g as orange crystal (59%). ¹H NMR (400 MHz, CDCl₃) δ 8.13 (d, J = 2.4, 1H, ArH), 8.10 (d, J = 8.8, 1H, ArH), 7.57 (dd, J₁ = 8.8, J₂ = 2.4, 1H, ArH), 2.40 (s, 3H, CH₃). ¹³C NMR (100 MHz, CDCl₃) δ 172.02, 169.05, 149.47, 143.04, 130.23, 129.60, 128.29, 126.90, 21.11.

4-bromo-2-(chlorocarbonyl)phenyl hypochloroselenoite (3h)

Compound 2h (5.6g, 0.01mol) was used as reactant to give 4.7g of 3h as yellow crystal (71%). ¹H NMR (400 MHz, CDCl₃) δ 8.14 (d, J = 2.2, 1H, ArH), 7.65 (dd, J₁ = 8.6, J₂ = 2.2, 1H, ArH), 7.49 (d, J = 8.6, 1H, ArH). ¹³C NMR (100 MHz, CDCl₃) δ 171.55, 145.11, 138.90, 136.60, 130.34, 128.70, 120.33.

General methods of the synthesis of 4(a,b,d,e,g)-(1-3), 4c-1, 4f-1, 4h-1

2-(chlorocarbonyl)phenyl hypochloroselenoite (0.01 mol) dissolved in 50 ml ether and N-Boc-ethylenediamine (0.015mol) was dropped into the mixture and stirred at room temperature for 3 h. Precipitation occurred and the filter residues redissolved in 10 ml methylene chloride. Trifluoroacetic acid (4 ml) was added in to the mixture slowly and stirred at room temperature for 40 min. Then, the pH was regulated with saturated aqueous Sodium Bicarbonate (10%) to a value of 7-8. The water

layer was obtain and enriched to 30 ml. The mixture was extracted by 100 ml methylene chloride for several times and the extracts were dried over anhydrous sodium sulfate overnight. After the desiccant was removed by filtration, the filtrate was concentrate to 10 ml. 2-Chloroethyl isocyanate (0.5 ml) was added slowly and stirred at 20°C for 30 min. After another filtration, the filter residues redissolved in anhydrous formic acid (2 ml) and cooled at 0°C. The reaction mixture was added sodium nitrite (0.04 mol) and stirred for 40 min at 0°C. After adding the water as needed into mixture, the final products were acquired by filtration.

1-(2-chloroethyl)-1-nitroso-3-(2-(3-oxobenzoselenazol-2(3H)-yl)ethyl)urea (4a-1)

Compound 3a (0.01 mol), N-Boc-ethylenediamine (0.015mol) and sodium nitrite (0.04 mol) were used as reactants to give 0.564 g of 4a-1 as white solid (15%). ¹H NMR (400 MHz, DMSO) δ 8.87 (t, J = 5.6 Hz, 1H), 8.01 (d, J = 8.0 Hz, 1H), 7.77 (d, J = 7.0 Hz, 1H), 7.66-7.52 (m, 1H), 7.41 (t, J = 7.1 Hz, 1H), 4.04 (t, J = 5.7 Hz, 2H), 3.76 (t, J = 5.6 Hz, 2H), 3.66-3.42 (m, 4H). MS (EI) m/z: 376.0 (M⁺).

1-(2-chloroethyl)-1-nitroso-3-(3-(3-oxobenzoselenazol-2(3H)-yl)propyl)urea (4a-2)

Compound 3a (0.01 mol), N-Boc-1,3-propylenediamine (0.015mol) and sodium nitrite (0.04 mol) were used as reactants to give 0.468 g of 4a-2 as white solid (12%). ¹H NMR (400 MHz, DMSO) δ 8.92 (t, J = 5.7 Hz, 1H), 8.05 (d, J = 8.0 Hz, 1H), 7.80 (d, J = 6.9 Hz, 1H), 7.62 (t, J = 7.6 Hz, 1H), 7.42 (t, J = 7.4 Hz, 1H), 3.85-3.78 (m, 2H), 3.76 (t, J = 6.3 Hz, 2H), 3.70-3.57 (m, 3H), 2.06-1.94 (m, 1H), 1.76-1.63 (m, 2H). MS (EI) m/z: 390.0 (M⁺).

1-(2-chloroethyl)-1-nitroso-3-(4-(3-oxobenzoselenazol-2(3H)-yl)butyl)urea (4a-3)

Compound 3a (0.01 mol), N-Boc-1,4-butanediamine (0.015mol) and sodium nitrite (0.04 mol) were used as reactants to give 0.364 g of 4a-3 as white solid (9%). ¹H NMR (400 MHz, DMSO) δ 8.91 (t, J = 5.5 Hz, 1H), 8.04 (d, J = 8.0 Hz, 1H), 7.79 (d, J = 6.8 Hz, 1H), 7.61 (t, J = 7.6 Hz, 1H), 7.42 (t, J = 7.0 Hz, 1H), 3.77 (dt, J = 12.8, 6.5 Hz, 3H), 3.68 (t, J = 6.9 Hz, 2H), 3.61 (dd, J = 12.2, 6.1 Hz, 2H), 2.04-1.93 (m, 1H), 1.54-1.43 (m, 2H), 1.36 (dd, J = 19.7, 12.8 Hz, 2H). MS (EI) m/z: 404.0 (M⁺).

1-(2-chloroethyl)-3-(2-(5-fluoro-3-oxobenzoselenazol-2(3H)-yl)ethyl)-1-nitrosourea (4b-1)

Compound 3b (0.01 mol), N-Boc-ethylenediamine (0.015mol) and sodium nitrite (0.04 mol) were used as reactants to give 0.512 g of 4b-1 as white solid (13%). ¹H NMR (400 MHz, DMSO) δ 8.88 (t, J = 5.6 Hz, 1H), 8.12-7.95 (m, 1H), 7.57-7.40 (m, 2H), 4.04 (t, J = 5.6 Hz, 2H), 3.76 (t, J = 5.6 Hz, 2H), 3.63 (t, J = 6.2 Hz, 2H), 3.54-3.43 (m, 2H). MS (EI) m/z: 393.9 (M⁺).

1-(2-chloroethyl)-3-(3-(5-fluoro-3-oxobenzoselenazol-2(3H)-yl)propyl)-1-nitrosourea (4b-2)

Compound 3b (0.01 mol), N-Boc-1,3-propylenediamine (0.015mol) and sodium nitrite (0.04 mol) were used as reactants to give 0.468 g of 4b-2 as white solid (12%).

¹H NMR (400 MHz, DMSO) δ 8.99-8.66 (m, 1H), 8.10 (dd, J = 8.6, 4.6 Hz, 1H), 7.61-7.28 (m, 2H), 3.81 (ddd, J = 22.4, 13.7, 7.2 Hz, 4H), 3.69-3.51 (m, 4H), 1.76-1.60 (m, 2H). MS (EI) m/z: 408.0 (M+).

1-(2-chloroethyl)-3-(4-(5-fluoro-3-oxobenzoselenazol-2(3H-yl)butyl)-1-nitrosoourea (4b-3)

Compound 3b (0.01 mol), N-Boc-1,4-butanediamine (0.015mol) and sodium nitrite (0.04 mol) were used as reactants to give 0.464 g of 4b-3 as white solid (11%). ¹H NMR (400 MHz, DMSO) δ 8.89 (t, J = 18.7 Hz, 1H), 8.17-7.98 (m, 1H), 7.52 (t, J = 8.9 Hz, 2H), 3.91-3.51 (m, 8H), 1.53-1.29 (m, 4H). MS (EI) m/z: 422.0 (M+).

1-(2-chloroethyl)-3-(2-(6-fluoro-3-oxobenzoselenazol-2(3H-yl)ethyl)-1-nitrosoourea (4c-1)

Compound 3c (0.01 mol), N-Boc-ethylenediamine (0.015mol) and sodium nitrite (0.04 mol) were used as reactants to give 0.355 g of 4a-7 as white solid (9%). ¹H NMR (400 MHz, DMSO) δ 8.86 (t, J = 5.6 Hz, 1H), 7.79 (dt, J = 8.5, 4.4 Hz, 2H), 7.34-7.17 (m, 1H), 4.03 (t, J = 5.6 Hz, 2H), 3.75 (t, J = 5.7 Hz, 2H), 3.62 (t, J = 6.3 Hz, 2H), 3.53 (dd, J = 12.1, 6.1 Hz, 2H). MS (EI) m/z: 394.0 (M+).

3-(2-(5-chloro-3-oxobenzoselenazol-2(3H-yl)ethyl)-1-(2-chloroethyl)-1-nitrosoourea (4d-1)

Compound 4d (0.01 mol), N-Boc-ethylenediamine (0.015mol) and sodium nitrite (0.04 mol) were used as reactants to give 0.409 g of 4d-1 as white solid (10%). ¹H NMR (400 MHz, CDCl₃) δ 8.01 (t, J = 4.6 Hz, 1H), 7.63-7.42 (m, 2H), 4.31-4.10 (m, 2H), 3.88 (dd, J = 15.2, 9.7 Hz, 2H), 3.83-3.70 (m, 2H), 3.64 (t, J = 5.6 Hz, 2H). MS (EI) m/z: 409.9 (M+).

3-(3-(5-chloro-3-oxobenzoselenazol-2(3H-yl)propyl)-1-(2-chloroethyl)-1-nitrosoourea (4d-2)

Compound 4d (0.01 mol), N-Boc-1,3-propylenediamine (0.015mol) and sodium nitrite (0.04 mol) were used as reactants to give 0.339 g of 4d-2 as white solid (8%). ¹H NMR (400 MHz, DMSO) δ 8.92 (s, 1H), 8.18-8.00 (m, 1H), 7.80-7.59 (m, 2H), 3.90-3.70 (m, 4H), 3.62 (dt, J = 12.8, 6.1 Hz, 4H), 2.05-1.87 (m, 2H). MS (EI) m/z: 424.0 (M+).

3-(4-(5-chloro-3-oxobenzoselenazol-2(3H-yl)butyl)-1-(2-chloroethyl)-1-nitrosoourea (4d-3)

Compound 4d (0.01 mol), N-Boc-1,4-butanediamine (0.015mol) and sodium nitrite (0.04 mol) were used as reactants to give 0.263 g of 4d-3 as white solid (6%). ¹H NMR (400 MHz, DMSO) δ 8.89 (dd, J = 21.6, 16.0 Hz, 1H), 8.04 (dd, J = 18.4, 8.6 Hz, 1H), 7.79-7.53 (m, 2H), 4.08 (t, J = 6.4 Hz, 1H), 3.87-3.51 (m, 6H), 2.00 (dd, J = 14.5, 6.8 Hz, 1H), 1.60-1.28 (m, 4H). MS (EI) m/z: 438.0 (M+).

3-(2-(6-chloro-3-oxobenzoselenazol-2(3H-yl)ethyl)-1-(2-chloroethyl)-1-nitrosoourea (4e-1)

Compound 4e (0.01 mol), N-Boc-ethylenediamine (0.015mol) and sodium nitrite (0.04 mol) were used as reactants to give 0.287 g of 4e-1 as white solid (7%). ¹H NMR (400 MHz, DMSO) δ 8.12 (d, J = 31.9 Hz, 1H), 7.54-7.41 (m, 1H), 7.21 (s, 1H), 6.67 (s, 1H), 3.68 (dd, J = 34.6, 28.6 Hz, 4H), 3.05 (t, J = 5.9 Hz, 2H), 2.63 (d, J

= 31.7 Hz, 2H). MS (EI) m/z: 410.0 (M+).

1-(2-chloroethyl)-3-(2-(5-methyl-3-oxobenzoselenazol-2(3H-yl)ethyl)-1-nitrosoourea (4f-1)

Compound 4f (0.01 mol), N-Boc-ethylenediamine (0.015mol) and sodium nitrite (0.04 mol) were used as reactants to give 0.429 g of 4f-1 as white solid (11%). ¹H NMR (400 MHz, DMSO) δ 8.87 (t, J = 5.4 Hz, 1H), 7.89 (t, J = 10.8 Hz, 1H), 7.61 (d, J = 19.9 Hz, 1H), 7.43 (d, J = 8.0 Hz, 1H), 4.03 (t, J = 5.6 Hz, 2H), 3.74 (t, J = 5.6 Hz, 2H), 3.68-3.57 (m, 2H), 3.53 (dd, J = 12.0, 6.0 Hz, 2H), 2.36 (d, J = 22.8 Hz, 3H). MS (EI) m/z: 390.0 (M+).

1-(2-chloroethyl)-3-(3-(5-methyl-3-oxobenzoselenazol-2(3H-yl)propyl)-1-nitrosoourea (4f-2)

Compound 4f (0.01 mol), N-Boc-1,3-propylenediamine (0.015mol) and sodium nitrite (0.04 mol) were used as reactants to give 0.362 g of 4f-2 as white solid (9%). ¹H NMR (400 MHz, DMSO) δ 8.91 (dd, J = 19.6, 14.3 Hz, 1H), 7.92 (d, J = 8.2 Hz, 1H), 7.67-7.54 (m, 1H), 7.44 (d, J = 8.3 Hz, 1H), 3.92-3.69 (m, 4H), 3.69-3.50 (m, 4H), 2.36 (d, J = 26.8 Hz, 3H), 1.68 (dd, J = 14.0, 7.0 Hz, 2H). MS (EI) m/z: 404.0 (M+).

1-(2-chloroethyl)-3-(4-(5-methyl-3-oxobenzoselenazol-2(3H-yl)butyl)-1-nitrosoourea (4f-3)

Compound 4f (0.01 mol), N-Boc-1,4-butanediamine (0.015mol) and sodium nitrite (0.04 mol) were used as reactants to give 0.294 g of 4f-3 as white solid (7%). ¹H NMR (400 MHz, DMSO) δ 8.89 (dd, J = 21.3, 15.6 Hz, 1H), 7.90 (dd, J = 16.5, 8.3 Hz, 1H), 7.72-7.56 (m, 1H), 7.41 (dt, J = 41.3, 20.7 Hz, 1H), 3.75 (dt, J = 28.9, 14.9 Hz, 4H), 3.62 (tt, J = 19.3, 6.4 Hz, 4H), 2.36 (d, J = 25.5 Hz, 3H), 1.59-1.44 (m, 2H), 1.36 (dt, J = 13.4, 6.6 Hz, 2H). MS (EI) m/z: 418.0 (M+).

1-(2-chloroethyl)-3-(2-(5-methoxy-3-oxobenzoselenazol-2(3H-yl)ethyl)-1-nitrosoourea (4g-1)

Compound 4g (0.01 mol), N-Boc-ethylenediamine (0.015mol) and sodium nitrite (0.04 mol) were used as reactants to give 0.320 g of 4g-1 as white solid (8%). ¹H NMR (400 MHz, DMSO) δ 8.89 (dd, J = 23.3, 17.5 Hz, 1H), 8.08 (dd, J = 26.5, 14.3 Hz, 1H), 7.78-7.58 (m, 2H), 4.18-3.98 (m, 2H), 3.74 (dt, J = 13.0, 5.8 Hz, 2H), 3.67-3.57 (m, 2H), 3.57-3.43 (m, 2H), 3.34 (s, 3H). MS (EI) m/z: 406.0 (M+).

1-(2-chloroethyl)-3-(3-(5-methoxy-3-oxobenzoselenazol-2(3H-yl)propyl)-1-nitrosoourea (4g-2)

Compound 4g (0.01 mol), N-Boc-1,3-propylenediamine (0.015mol) and sodium nitrite (0.04 mol) were used as reactants to give 0.256 g of 4g-2 as white solid (6%). ¹H NMR (400 MHz, DMSO) δ 8.92 (t, J = 5.6 Hz, 1H), 7.91 (d, J = 8.7 Hz, 1H), 7.27 (ddd, J = 11.5, 7.9, 3.6 Hz, 2H), 3.85-3.71 (m, 6H), 3.69-3.55 (m, 4H), 2.05-1.95 (m, 1H), 1.75-1.62 (m, 2H). MS (EI) m/z: 420.0 (M+).

1-(2-chloroethyl)-3-(4-(5-methoxy-3-oxobenzoselenazol-2(3H-yl)butyl)-1-nitrosoourea (4g-3)

Compound 4g (0.01 mol), N-Boc-1,4-butanediamine (0.015mol) and sodium nitrite (0.04 mol) were used as reactants to give 0.174 g of 4g-3 as white solid (4%). ¹H NMR (400 MHz, DMSO) δ 8.91 (s, 1H), 7.90 (d, J = 8.6

H_z, 1H), 7.37-7.19 (m, 2H), 3.93-3.71 (m, 5H), 3.70-3.55 (m, 3H), 2.33 (s, 1H), 2.05-1.94 (m, 2H), 1.47 (m, 2H), 1.39 (m, 2H). MS (EI) m/z: 434.0 (M⁺).

3-(2-(5-bromo-3-oxobenzoselenazol-2(3H)-yl)ethyl)-1-(2-chloroethyl)-1-nitroso-urea (4h-1)

Compound 4h (0.01 mol), N-Boc-ethylenediamine (0.015 mol) and sodium nitrite (0.04 mol) were used as reactants to give 0.273 g of 4h-1 as white solid (6%). ¹H NMR (400 MHz, DMSO) δ 8.86 (s, 1H), 7.97 (d, J = 8.5 Hz, 1H), 7.91-7.83 (m, 1H), 7.77 (dd, J = 8.6, 2.1 Hz, 1H), 4.05 (dd, J = 10.5, 5.5 Hz, 2H), 3.82-3.70 (m, 2H), 3.62 (t, J = 6.1 Hz, 2H), 3.53 (d, J = 5.8 Hz, 2H). MS (EI) m/z: 453.9 (M⁺).

Biological experiments

Rat liver Thioredoxin reductase was obtained by using the method of Luthman and Holmgren (25). DTNB were bought from Sigma–Aldrich. Carmustin (BCNU) were obtained from Sigma, USA. Ethaselen (PCT: CN02-00413) was prepared in our laboratory (School of Pharmaceutical Sciences, Peking University, Beijing, China). Human colonic adenocarcinoma RKO cell lines (ATCC number: CRL-2577) and LoVo cell lines (ATCC number: CCL-229) were purchased from American Type Culture Collection (ATCC). Parental pancreatic carcinoma MIA PaCa-2 cell lines and PANC-1 cell lines were obtained from Chinese Academy of Medical Sciences.

Solubility studies

According to the European Pharmacopoeia, put 100 mg finely powdered Ethaselen, 4a-1, 4c-1 in a stoppered tube, respectively, and each one added a specific volume (0.1, 1, 3, 10, 100, 1000 ml) of different solvents. Shake the tube vigorously for 1 min at a temperature of 25.0 ± 0.5 °C for 15 min. If the substance is not completely dissolved, repeat the shaking for 1 min. The solubility was determined based on whether the compound dissolved completely in different volume level.

Toxicity studies

KM mice (5-week-old, male) were used in the assays. Under the condition of 25 ± 2 °C, all mice were freely to get food and water in SPF condition. Mice were distributed into three groups equally and randomly: control (with saline), carmustine group (with carmustine alone, 30 mg/kg, i.v. on days 0, 4, 8, 12), 4a-1 group (receiving 4a-1 alone, 36 mg/kg, i.v. on days 0, 4, 8, 12). The assays were carried out according to the guidelines and notes of the Ethical Committee of Peking University.

Cell culture and cell growth inhibitory assays

All cells were obtained from the Beijing Institute of Cancer Research. Human cancer cell lines PANC-1 cells, MIA PaCa-2 cells, RKO cells grew in DMEM medium and LoVo cells in RPMI 1640 medium supplemented with 10% fetal bovine serum (FBS) in 5% CO₂ atmosphere at 37 °C. Cells in the exponential growth phase were then plated into 96-well plates at 5000 cells/well. After exposure to various concentrations (0–50 μM) of these compounds for 48 h. The growth inhibition activities of representative compounds on human cancer cell lines were determined using the 3-(4,5-dimethylthiazol-

2-yl)-2,5-diphenyltetrazolium bromide (MTT) assay.

Cellular TrxR inhibition assays

Representative compounds with different concentrations were added into the MIA PaCa-2 cells while DMSO (1%) as control and incubated for 12 h. Washed by phosphate saline buffer, the cells were subsequently lysed using lysing buffer 1% Triton X-100, 1% NaDOC, 10 mM EDTA, 0.1% sodium dodecyl sulfate and 0.5 mM phenylmethylsulfonyl fluoride and then centrifuged at 13000g for 30 min at 4 °C. Cellular TrxR activities were detected by reducing insulin method. After the control value (without E. coli Trx) subtraction, TrxR activities were calculated.

Molecular docking assays

Human thioredoxin reductase 1 (PDB code: 2J3N) structure was downloaded from Brookhaven Protein Database. The docking procedure was conducted in Discovery Studio 2.5. The receptor protein employed the prepare protein procedure. After removing the crystallized water and adding hydrogen atoms, the molecular structure was typed using CHARMM forcefield. The ligand (4b-1) was put into TrxR key active cavity by the method of CDOCKER. The active sphere within 15 Å embraced with the redox-active centers of TrxR, including Cys 497, Sec 498, Cys 59 and Cys 64. Ten top hits runs were set in the docking function. Then, the ligand interaction diagram was drawn to indicate the interaction more directly by the 2D picture.

Results and Discussion

Design and chemistry

Association strategies are adopted in the drug design in order to combine the effects of TrxR inhibition and DNA crosslink within one compound. 4a-1 and its analogues were first designed and synthesized by our group. The core 1-(2-chloroethyl)-1-nitroso-3-(2-(3-oxobenzoselenazol-2(3H)-yl)ethyl)urea structure was kept and focused predominantly on addition of some substituents on aromatic rings because 4a-1 was designed to contain two active sites exerting different effects inhibiting Sec498 residues of TrxR, binding to the lys-protein, DNA cross-linking. To develop potent analogues of 4a-1 with better antitumor properties and to understand the SAR of 1-(2-chloroethyl)-1-nitroso-3-(2-(3-oxobenzoselenazol-2(3H)-yl)ethyl)urea as a novel multi-target candidate, a series of substituted 1-(2-chloroethyl)-1-nitroso-3-(2-(3-oxobenzoselenazol-2(3H)-yl)ethyl)urea were designed and synthesized.

In the reaction scheme, as shown in figure 2, the first two steps can react to form 3a-3h with relatively high yields. While it was difficult to isolate the free diamine to react with 2-Chloroethyl isocyanate in order to form the backbone, Boc-protected amino groups were introduced into the backbone chains by 3a-3h ring closing with N-Boc-ethylenediamine. After removal of the Boc groups by Trifluoroacetic acid, amine groups were produced on the backbones. Because of the low yields and separation difficulty of the products of step 3-5, the products of each step were put into the next step without further separation and purification until the target product was obtained.

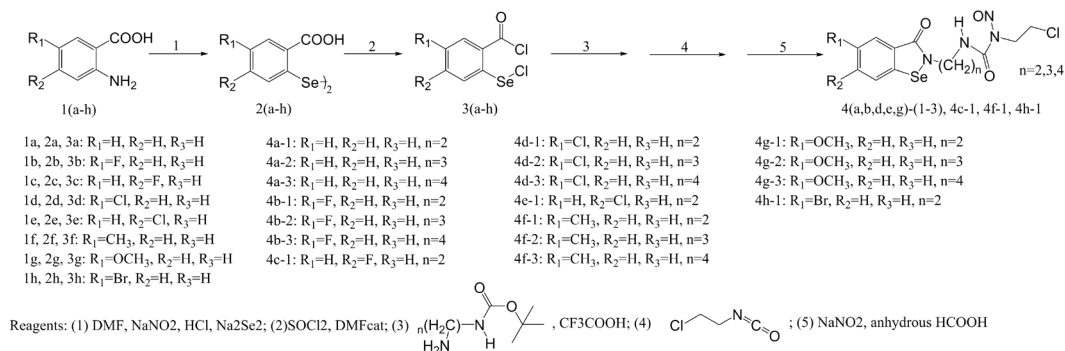


Figure 2. The schemes of the target compounds synthesis.

Solubility studies

Ethaselen, a novel organoselenium compound inhibiting TrxR1, showed huge potential as a targeted antitumor candidate. However, the unsatisfactory solubility due to its symmetrical structure may limit its clinical application to some extents. By combining the active sites of ethaselen and carmustine, the backbone was modified into unsymmetrical structure, namely 1-(2-chloroethyl)-1-nitroso-3-(2-(3-oxobenzoselenazol-2(3H)-yl)ethyl)urea. The new designed compounds showed better solubility in most solvents as showed in table 1.

Toxicity studies

In order to assess the toxicity of new designed compounds, the change of body weight is introduced as an important index to detect systemic toxicity. Despite transient weight loss after drug treatment, as shown in Figure 3, the 4a-1 group showed not significant ($P > 0.05$) effect over 24 days compared to the control group, whereas there was a marked tendency of body weight declining in the carmustine group compared with control group, showing significant ($P < 0.05$) difference. As compared to carmustine, 4a-1 appeared to be somewhat less toxic, which may partly result from the good targeting and selectivity by introducing the structure of benzoselenazol-3(2H)-ones into the new designed backbone. After stopping administration, the body weight of both carmustine group and 4a-1 group had a certain degree of recovery.

Cell growth inhibition assay

In order to study the antitumor activity of the novel

antitumor compounds, the inhibitory activities of the novel compounds on RKO cells (colon cancer), LoVo cells (colon cancer), PANC-1 cells (pancreatic carcinoma), MIA PaCa-2 cells (pancreatic carcinoma) were examined, as shown in table 2. As expected, good inhibitory activities can be observed in all tested cell lines incubated with these compounds, of which compound 4b-1 and 4c-1 showed the strongest antitumor effect. However, compounds with chloro or bromo substituents (4d-1, 4d-2, 4d-3, 4e-2, 4h-1) exhibited relatively low inhibitory activities on cancer cells, whereas the fluoro analogues (4b-1, 4b-2, 4b-3, 4c-1) were much more active in all tested cells (table 2). In addition, the increased lengths of alkyl chains (n from 2 to 4) leads to less inhibitory activity. Subsequent calculation of CLogP values for these synthesized compounds, revealed a tendency that smaller CLogP may lead to better antitu-

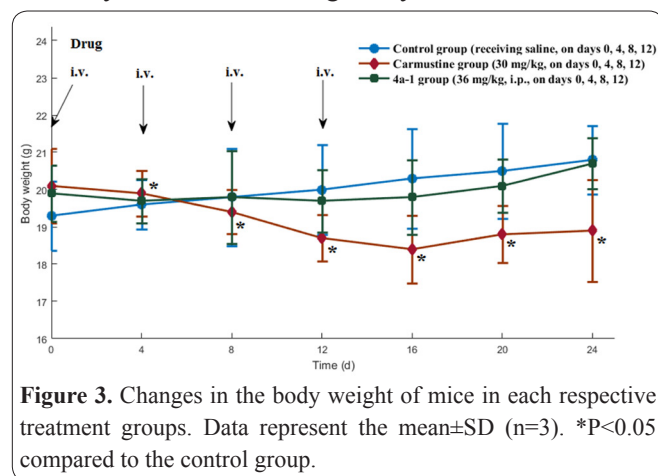


Figure 3. Changes in the body weight of mice in each respective treatment groups. Data represent the mean \pm SD ($n=3$). * $P < 0.05$ compared to the control group.

Table 1. The solubility of Ethaselen, 4a-1, 4c-1 in common solvents.

| | Ethaselen | 4a-1 | 4c-1 |
|--------------------|-----------------------|----------------|----------------|
| water | insoluble | Soluble | Freely soluble |
| petroleum ether | insoluble | Soluble | Soluble |
| Ether | insoluble | Soluble | Soluble |
| methylene chloride | Very slightly soluble | Freely soluble | Freely soluble |
| acetonitrile | Slightly soluble | Freely soluble | Freely soluble |
| ethanol | Very slightly soluble | Soluble | Freely soluble |
| tetrahydrofuran | Very slightly soluble | Soluble | Freely soluble |
| chloroform | Slightly soluble | Freely soluble | very soluble |
| ethyl acetate | Very slightly soluble | Freely soluble | Freely soluble |
| methanol | Slightly soluble | Freely soluble | very soluble |
| acetone | Slightly soluble | Freely soluble | very soluble |
| DMF | Slightly soluble | Very soluble | very soluble |
| DMSO | Sparingly soluble | Very soluble | very soluble |

Table 2. Growth inhibition of the novel compounds^a.

| Compound | R1 | R2 | n | CLogP | IC50 (μM) of cell lines | | | |
|----------|------|----|---|-------|-------------------------|------------|------------|------------|
| | | | | | Mia PaCa-2 | PANC-1 | RKO | LoVo |
| 4a-1 | H | H | 2 | 2.616 | 16.33±1.5 | 7.78±0.36 | 12.24±0.44 | 7.29±0.98 |
| 4a-2 | H | H | 3 | 2.927 | 12.33±0.58 | 7.52±1.09 | 10.9±1.01 | 7.62±1.17 |
| 4a-3 | H | H | 4 | 3.047 | 11.9±0.78 | 7.78±0.78 | 11.25±1.66 | 12.12±1.82 |
| 4b-1 | F | H | 2 | 2.759 | 3.39±0.76 | 6.13±0.31 | 8.43±0.84 | 5.49±0.33 |
| 4b-2 | F | H | 3 | 3.07 | 12.89±1.38 | 14.36±2.14 | 20.54±3.24 | 13.87±1.11 |
| 4b-3 | F | H | 4 | 3.19 | 25.3±3.49 | 14.43±1.49 | 17.17±2.33 | 13.25±0.96 |
| 4c-1 | H | F | 2 | 2.759 | 8.17±0.65 | 2.61±0.27 | 5.46±0.85 | 2.62±0.26 |
| 4d-1 | Cl | H | 2 | 3.329 | 27.36±2.5 | 18.9±0.6 | 15.92±1.74 | 14.78±0.26 |
| 4d-2 | Cl | H | 3 | 3.64 | >50 | 34.24±3.47 | >50 | 28.57±0.95 |
| 4d-3 | Cl | H | 4 | 3.76 | >50 | >50 | 29.39±1.37 | 37.37±2.23 |
| 4e-1 | H | Cl | 2 | 3.329 | >50 | 23.95±3.16 | 22.54±2.53 | 35.56±1.8 |
| 4f-1 | CH3 | H | 2 | 3.115 | 20.4±2.22 | 9.41±1.45 | 8.63±0.47 | 8.02±0.81 |
| 4f-2 | CH3 | H | 3 | 3.426 | 9.82±1.27 | 7.14±0.54 | 14.21±1.91 | 16.67±1.43 |
| 4f-3 | CH3 | H | 4 | 3.546 | 13.44±0.96 | 8.23±0.91 | 15.8±2.5 | 17.7±0.81 |
| 4g-1 | OCH3 | H | 2 | 2.535 | 11.61±1.15 | 11.33±0.4 | 18.75±2.14 | 9.77±0.8 |
| 4g-2 | OCH3 | H | 3 | 2.846 | 10.87±0.88 | 12.58±0.91 | 11.44±1.14 | 10.56±1.26 |
| 4g-3 | OCH3 | H | 4 | 2.966 | 24.57±2.73 | 39.26±1.34 | 22.17±1.78 | 31.06±1.66 |
| 4h-1 | Br | H | 2 | 3.479 | >50 | >50 | >50 | 40.64±1.03 |

a. All data are shown in IC50 (μM) values and expressed as means ± SD of triplicate experiments.

Table 3. The correlation coefficient of growth inhibitory activities and CLogP of these compounds.

| Cell lines | Correlation Coefficient (r) ^a |
|------------|--|
| Mia PaCa-2 | 0.695 |
| PANC-1 | 0.271 |
| RKO | 0.606 |
| LoVo | 0.662 |

^aThe values of r were represented by Pearson coefficient.

mor effect, which had a medium correlation in statistics except for PANC-1 cell lines, as shown in table 3. The decreased antitumor activities of some compounds may result from the hinder cellular permeability due to the high lipophilicity (large LogP).

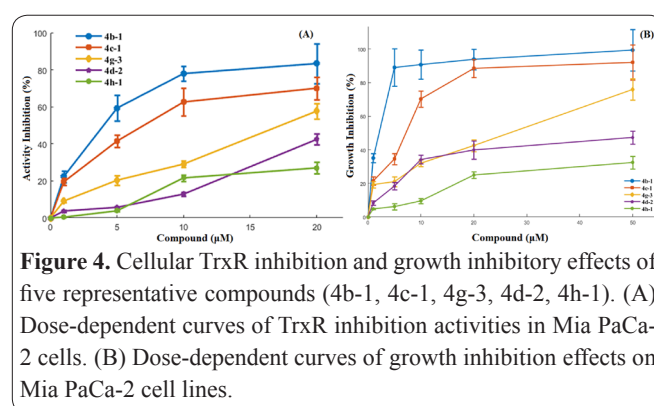
Cellular TrxR inhibition assay

In order to conform that the TrxR is still a major target of these new compounds after combination of ethaselen and carmustine. The links between TrxR inhibition and antitumor activities of these novel compounds was investigated and the correlation was further calculated. Five representative compounds (4b-1, 4c-1, 4g-3, 4d-2, 4h-1) with different antitumor effects were selected to study the inhibitory effects on Mia PaCa-2 cell lines. After exposure to 1-20 μM solutions of some representative compounds, the TrxR activities were declined to different levels, as shown in figure 4. Compared with growth inhibition, according to the correlation coefficients in table 4, a strong correlation was revealed, which means the better cell growth inhibition resulting in the higher percentile inhibition of intracellular TrxR

Table 4. The correlation of growth inhibition and TrxR inhibition.

| Compounds | Correlation Coefficient (r) ^a |
|-----------|--|
| 4b-1 | 0.97 |
| 4c-1 | 0.97 |
| 4g-1 | 0.93 |
| 4d-2 | 0.83 |
| 4h-1 | 0.87 |

^aThe values of r were represented by pearson coefficient.

**Figure 4.** Cellular TrxR inhibition and growth inhibitory effects of five representative compounds (4b-1, 4c-1, 4g-3, 4d-2, 4h-1). (A) Dose-dependent curves of TrxR inhibition activities in Mia PaCa-2 cells. (B) Dose-dependent curves of growth inhibition effects on Mia PaCa-2 cell lines.

and vice versa. The compound 4b-1 were the best both at inhibiting the cell growth and cellular TrxR in the five selected compounds. This may be a strong evidence indicating TrxR as a major target of these novel compounds.

Computational docking Study

To further explore the pattern of interaction between these compounds and TrxR and to conduct further SARs study, the docking study was carried out with 4a-1 and crystallographic structure of TrxR. The sphere cavity with the two redox-active centers (Cys59, Cys64, Cys497 and Sec498) was created. As shown in figure 5 and 6, the formation of three hydrogen bonds was observed, including oxygen of 4a-1 and hydrogen of Arg351, oxygen of 4a-1 and hydrogen of Lys29, nitrogen of 4a-1 and hydrogen of Lys29. The docking results showed one unit of 4a-1 inserted into the cavity consisting of Lys29, His108, Leu112, Tyr116, Arg351, Trp407, Leu409, His472, Cys497 and Sec498. It was demonstrated (20-22) that Trp407, His472, Lys29 and Tyr116 plays a key role for catalytic effects of TrxR through facilitating its reduction. Along with the correlation coefficient of inhibition effects of TrxR enzyme and cell growth, this results suggested that compound 4a-1 is a potential inhibitor of TrxR.

SAR model

In figure 7, the SARs for the series of novel

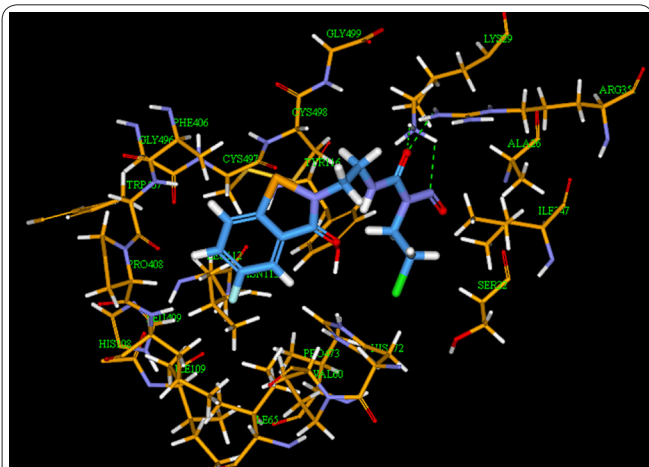


Figure 5. Docking models of compound 4b-1 in the cavity with the redox-active centers of TrxR. The ligand and residues are displayed as sticks. Hydrogen, white; carbons in residues, yellow; carbons in residues, blue; oxygen, red; nitrogen, purple; Chlorine, green; selenium orange; Hydrogen bonds between ligands and residues, green dash lines.

1-(2-chloroethyl)-1-nitroso-3-(2-(3-oxobenzoelenazol-2(3H)-yl)ethyl)urea as inhibitors of TrxR is established based on biological experiments and computational docking studies. The benzisoselenazolone heterocycle is essential for activity and targetability. Furthermore, small and polar substituents on the aromatic ring are preferred. The alkyl chain of the structure of benzisoselenazolone heterocycle and structure of 1-(2-chloroethyl)-1-nitrosourea prefers to be short. In addition, 1-(2-chloroethyl)-1-nitrosourea is essential for antitumor activity and H bond binding to the TrxR enzyme active sites. Encouragingly, the design of 4b-1 substantiates the assertion that structural modification of 4a-1 was necessary and workable to strengthen the biological activities of these new compounds.

Pharmacological mechanism hypothesis

Carmustine decomposes chemically under physiological conditions to yield 2-chloroethyl isocyanate and the chloroethyl carbonium ion intermediate, which is believed to be the alkylating moiety (23). Carmustine

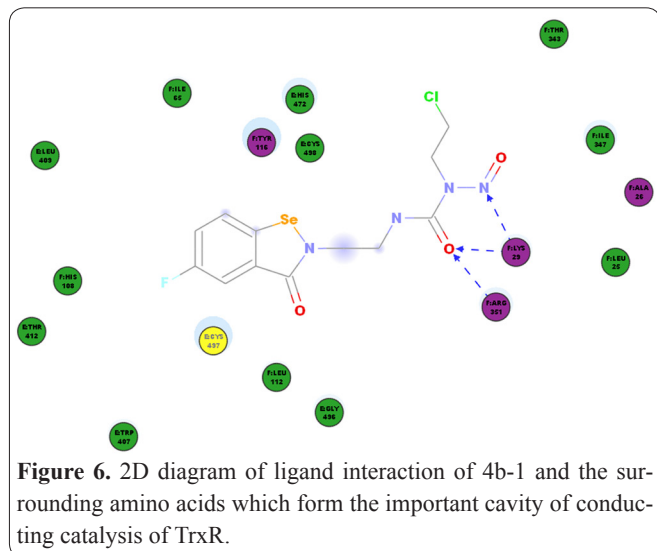


Figure 6. 2D diagram of ligand interaction of 4b-1 and the surrounding amino acids which form the important cavity of conducting catalysis of TrxR.

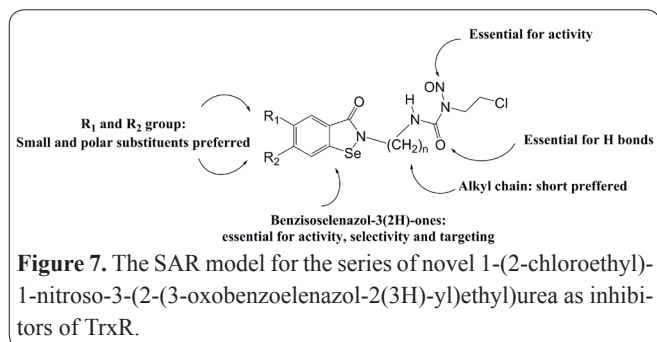


Figure 7. The SAR model for the series of novel 1-(2-chloroethyl)-1-nitroso-3-(2-(3-oxobenzoelenazol-2(3H)-yl)ethyl)urea as inhibitors of TrxR.

exerts anticancer activity via interstrand DNA cross-linking within a guanine-cytosine DNA base pair (13). Also, camustine which is capable of releasing amino-reactive 2-chloroethyl isocyanate can act almost exclusively on lysyl residues in proteins (24).

Hence, as shown in Figure 8, we hypothesized that the series of novel 1-(2-chloroethyl)-1-nitroso-3-(2-(3-oxobenzoelenazol-2(3H)-yl)ethyl)urea may decompose chemically under physiological conditions to yield a series of 2-(2-isocyanatoethyl)benzoselenazol-3(2H)-one (X) with Protein combination and TrxR inhibition and chloroethyl carbonium ion intermediate (Y). The series of 2-(2-isocyanatoethyl)benzoselenazol-3(2H)-one can inhibit TrxR for their benzisoselenazol-3(2H)-

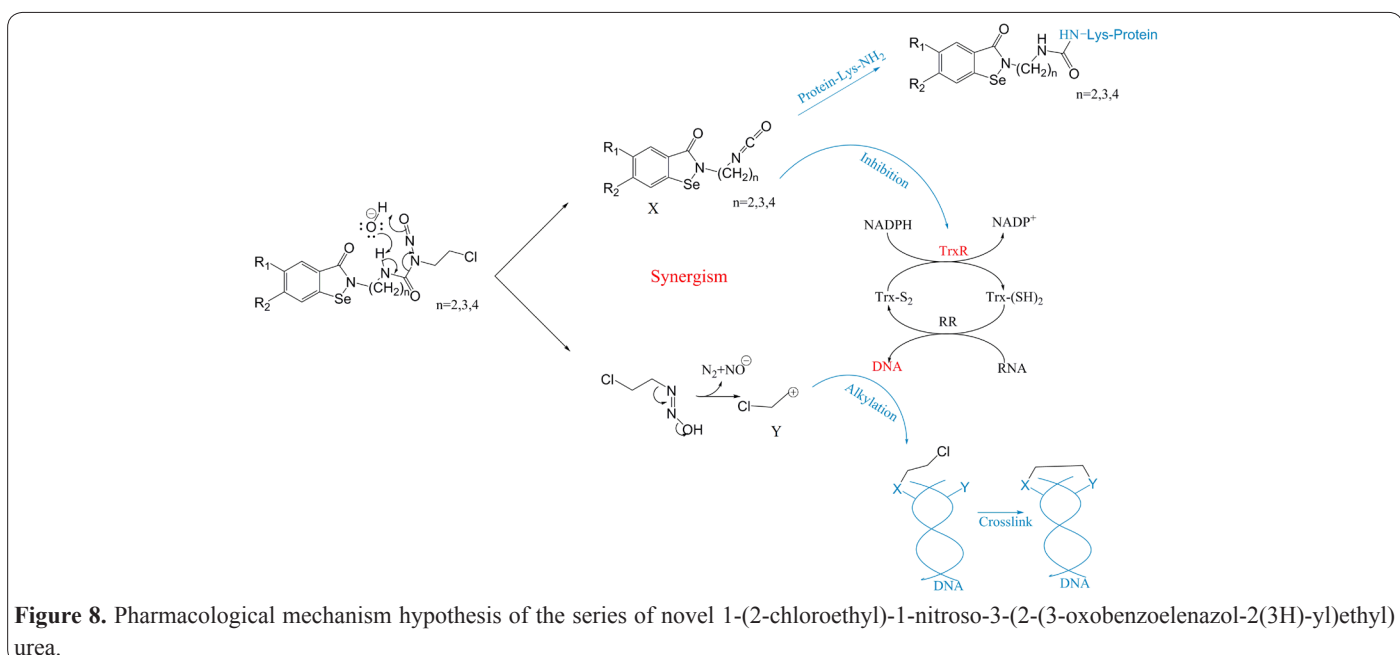


Figure 8. Pharmacological mechanism hypothesis of the series of novel 1-(2-chloroethyl)-1-nitroso-3-(2-(3-oxobenzoelenazol-2(3H)-yl)ethyl)urea.

one structures which are essential for the inhibition. Therefore, with the synergism in mechanism, these new compounds exert antitumor activities by the series of 2-(2-isocyanatoethyl)benzoselenazol-3(2H)-ones with TrxR inhibition and protein combination and the chloroethyl carbonium ion intermediate with DNA crosslinking effect. This hypothesis still needs further studies.

Acknowledgements

This work was supported in part by the National Natural Science Foundation [81372266] and National Science and Technology Major Project, People's Republic of China (2011zx09101-001-03).

References

1. Yoo MH, Xu XM, Carlson BA, Gladyshev VN, Hatfield DL. Thioredoxin reductase 1 deficiency reverses tumor phenotype and tumorigenicity of lung carcinoma cells. *J Biol Chem* 2006; 281 (19): 13005-8.
2. Gromer S, Eubel JK, Lee BL, Jacob J. Human selenoproteins at a glance. *Cell Mol Life Sci* 2005; 62 (21): 2414-37.
3. Engman L, Al-Maharik N, McNaughton M, Birmingham A, Powis G. Thioredoxin reductase and cancer cell growth inhibition by organotellurium compounds that could be selectively incorporated into tumor cells. *Bioorg Med Chem* 2003; 11 (23): 5091-100.
4. Grogan TM, Fenoglio-Prieser C, Zeheb R, Bellamy W, Frutiger Y, Vela E, *et al.* Thioredoxin, a putative oncogene product, is overexpressed in gastric carcinoma and associated with increased proliferation and increased cell survival. *Human Pathology* 2000; 31 (4): 475-81.
5. Smart DK, Ortiz KL, Mattson D, Bradbury CM, Bisht KS, Sieck LK, *et al.* Thioredoxin reductase as a potential molecular target for anticancer agents that induce oxidative stress. *Cancer Res* 2004; 64 (18): 6716-24.
6. Arner ES. Focus on mammalian thioredoxin reductases--important selenoproteins with versatile functions. *Biochim Biophys Acta* 2009; 1790 (6): 495-526.
7. Fang J, Lu J, Holmgren A. Thioredoxin reductase is irreversibly modified by curcumin: a novel molecular mechanism for its anticancer activity. *J Biol Chem* 2005; 280 (26): 25284-90.
8. Zhao F, Yan J, Deng SJ, Lan LX, He F, Kuang B, *et al.* A thioredoxin reductase inhibitor induces growth inhibition and apoptosis in five cultured human carcinoma cell lines. *Cancer Letters* 2006; 236 (1): 46-53.
9. Xing FX, Li SL, Ge XY, Wang CY, Zeng HH, Li D, *et al.* The inhibitory effect of a novel organoselenium compound BBSKE on the tongue cancer Tca8113 in vitro and in vivo. *Oral Oncology* 2008; 44 (10): 963-69.
10. Wang L, Fu JN, Wang JY, Jin CJ, Ren XY, Tan Q, *et al.* Selenium-containing thioredoxin reductase inhibitor ethaselen sensitizes non-small cell lung cancer to radiotherapy. *Anti-Cancer Drugs* 2011; 22 (8): 732-40.
11. He J, Li DD, Xiong K, Ge YJ, Jin HW, Zhang GZ, *et al.* Inhibition of thioredoxin reductase by a novel series of bis-1,2-benzisoseleazol-3(2H)-ones: Organoselenium compounds for cancer therapy. *Bioorganic & Medicinal Chemistry* 2012; 20 (12): 3816-27.
12. Li X, Yang Z, Yang K, Zhou Y, Chen X, Zhang Y, *et al.* Self-assembled polymeric micellar nanoparticles as nanocarriers for poorly soluble anticancer drug ethaselen. *Nanoscale Res Lett* 2009; 4 (12): 1502-11.
13. Egyhazi S, Bergh J, Hansson J, Karran P, Ringborg U. Carmustine-induced toxicity, DNA crosslinking and O6-methylguanine-DNA methyltransferase activity in two human lung cancer cell lines. *Eur J Cancer* 1991; 27 (12): 1658-62.
14. Rice KP, Klinkerch EJ, Gerber SA, Schleicher TR, Kraus TJ, Buros CM. Thioredoxin reductase is inhibited by the carbamoylating activity of the anticancer sulfonylhydrazine drug laromustine. *Mol Cell Biochem* 2012; 370 (1-2): 199-207.
15. Corti A, Ferrari SM, Lazzarotti A, Del Corso A, Mura U, Casini AF, *et al.* UV light increases vitamin C uptake by bovine lens epithelial cells. *Mol Vis* 2004; 10: 533-6.
16. Witte AB, Anestal K, Jerremalm E, Ehrsson H, Arner ES. Inhibition of thioredoxin reductase but not of glutathione reductase by the major classes of alkylating and platinum-containing anticancer compounds. *Free Radic Biol Med* 2005; 39 (5): 696-703.
17. Chrousos GA, Oldfield EH, Doppman JL, Cogan DG. Prevention of ocular toxicity of carmustine (BCNU) with supraorbital intracarotid infusion. *Ophthalmology* 1986; 93 (11): 1471-5.
18. Miller DF, Bay JW, Lederman RJ, Purvis JD, Rogers LR, Tomsak RL. Ocular and orbital toxicity following intracarotid injection of BCNU (carmustine) and cisplatin for malignant gliomas. *Ophthalmology* 1985; 92 (3): 402-6.
19. Shingleton BJ, Bienfang DC, Albert DM, Ensminger WD, Chandler WF, Greenberg HS. Ocular toxicity associated with high-dose carmustine. *Arch Ophthalmol* 1982; 100 (11): 1766-72.
20. Fritz-Wolf K, Urig S, Becker K. The Structure of Human Thioredoxin Reductase 1 Provides Insights into C-terminal Rearrangements During Catalysis. *Journal of Molecular Biology* 2007; 370 (1): 116-27.
21. Gromer S, Wessjohann LA, Eubel J, Brandt W. Mutational studies confirm the catalytic triad in the human selenoenzyme thioredoxin reductase predicted by molecular modeling. *ChemBioChem* 2006; 7 (11): 1649-52. English.
22. Cheng Q, Sandalova T, Lindqvist Y, Arnér ESJ. Crystal structure and catalysis of the selenoprotein thioredoxin reductase 1. *Journal of Biological Chemistry* 2009; 284 (6): 3998-4008.
23. Ren S, Slatterly JT. Inhibition of carboxyethylphosphoramidate mustard formation from 4-hydroxycyclophosphamide by carmustine. *AAPS PharmSci* 1999; 1 (3): E14.
24. Mann DM, Vanaman TC. Modification of calmodulin on Lys-75 by carbamoylating nitrosoureas. *J Biol Chem* 1988; 263 (23): 11284-90.
25. Luthman M, Holmgren A. Rat liver thioredoxin and thioredoxin reductase: purification and characterization. *Biochemistry* 1982; 21 (26): 6628-33.